Facile synthesis of hydrodynamic solid lubricant MoS_2 from molybdenum trioxide nanorods

Malayil Gopalan Sibi,[b] Bharat Singh Rana,[b] Lakshmi Narayana Sivakumar Konathala,[b] Gananath D. Thakre,[b] S. Saran,[b] and Anil Kumar Sinha[a),b]
Catalytic Conversion and Process Division, CSIR-Indian Institute of Petroleum, Dehradun 248005, India

(Received 8 March 2013; accepted 5 June 2013)

Molybdenum trioxide nanostructures were synthesized, to make highly friction resistant molybdenum disulfide, by low temperature hydrothermal reaction without using any template or catalyst. The as-synthesized materials were sulfided with H_2S at 400 and 800 °C. X-ray diffraction, scanning electron microscopy, transmission electron microscopy, Fourier-transform infra-red spectroscopy, and thermogravimetric analysis were used for the physical characterization of the materials. The oxide material is highly crystalline with unique morphology. The factors affecting the size and shape of the synthesized materials were studied in detail. The crystalline nature of the materials decreased after the sulfidation process at 800 °C without any change in morphology. The wear resistance and lubricity of the material were studied under harsh conditions. The comparative study of these materials with MoS_2 prepared by the hard templating method (using mesoporous silica template) reveals that the new material synthesized by direct hydrothermal route is pure phase and has better wear resistance and antifriction properties. Ultra high stability of the material is the most distinguished property of the material synthesized.

I. INTRODUCTION

Nanotechnology can produce materials having novel structures with unique function and utility, which is the driving force for research in this area of material science and engineering. In recent years, quasi one-dimensional nano-scaled materials have attracted attention both in academy and industry due to their potential applications in various fields like catalysis,[1–3] gas sensing,[4] electrochemistry[5,6] adsorption,[7] fuel cells,[8,9] solid lubricants,[10–12] etc. These materials are stronger, more dent resistant, have higher ductility, are lighter, and also have a host of other enhanced material characteristics, making them different from their bulk counterparts.[13–15] The chemical and physical properties of the materials at nanoscopic scale give a new perspective for the synthesis of new materials. Some of the more prominent materials in these classes are the oxides and sulfides of transition metals.[16–19] Due to the structural anisotropy, these are promising materials that need to be explored more for wider application in bulk scale.[20] The synthesis of nanomaterials with controlled shapes like rods, tubes, belts, etc. is usually done using high temperature complex reactions.

Transition metal oxides are an attractive group of materials due to their unusual chemistry produced by multiple valence states. Especially molybdenum-based materials possess stable coordination environments with unique functional properties, and due to which, these have been widely used in petroleum refining and petrochemical industries. Molybdenum trioxide materials have two polytypic phases: a thermodynamically stable orthorhombic phase and a metastable monoclinic phase,[21] and their nanostructures were extensively investigated and applied in various fields like gas sensors, Li-ion batteries,[22] catalysts,[23] etc. Substantial advancements have been achieved by a number of research groups to obtain controlled morphology of molybdenum nanostructures. Currently, these materials are synthesized by various methods like conventional hydrothermal processes, thermal evaporation, mechanical exfoliation, atmospheric micro-plasma deposition, template-assisted hydrothermal reaction, sonochemical process, RF magnetron sputtering, etc.[24–28] Most of these methods are complicated and high-temperature reactions. Also, the materials hence obtained have low homogeneity, and it is difficult to meet the requirements for large-scale synthesis. Due to the simplicity and ease of preparation, solution-based hydrothermal route has high importance to obtain homogeneous products of controlled morphology in a large scale.

Molybdenum disulfide is a class of transition metal dichalcogenide having a diagonal prismatic structure formed by stacking sandwiches consisting of a layer of transition metals held between layers of sulfur atoms by van der Waals forces.[5,12,15,20] It is widely used in a supported form in petroleum refining industry as a catalyst, in an unsupported form as an additive in liquid paraffin and as a solid lubricant in tribological field, where liquid lubricants are inapplicable. Since it has a layered structure

[a)]Address all correspondence to this author.
e-mail: asinha@iip.res.in
[b)]These authors contributed equally to this work.
DOI: 10.1557/jmr.2013.178

 © Materials Research Society 2013

https://doi.org/10.1557/jmr.2013.178 Published online by Cambridge University Press

that shears easily under sliding contact, giving rise to low coefficient of friction,[10] the lubrication performance of micro and nano-sized MoS_2 often exceeds that of graphite and is very effective in high temperature vacuum environments. Prevention of oxidation and intercrystallite slip is an added advantage of solid lubricants.[29] The presence of curved hexagonal planes enhances the stability of the material in humid environments and it helps to prevent the distortion of the lamellar structure.[30] Due to this, the solid lubricant can carry load and prevent direct metal–metal contact. Moreover, its use in the powder form can increase the efficiency of antifriction and antiwear capacities, which is its most vital advantage. But synthesis of anisotropic structures of the dichalcogenides with a controlled phase structure is a challenge. Various methods have been used for the synthesis of MoS_2 like thermal decomposition, solid state reaction, gas-phase reaction, pulsed laser deposition, microwave irradiation, hard template method, etc.,[24–29] either in single step with molybdenum and sulfur precursors or by multistep. The materials obtained in single step have sintered nature with high crystallinity, large grain size and, the morphology of the materials is difficult to control.

The characteristics giving these materials superior activity are reduced particle size with special morphology. Investigation of factors affecting the control of size and shape is important to obtain the material with desired dimension and morphology. Here, we report a simple hydrothermal route for the synthesis of micro- and nano-sized molybdenum oxide rods, flowers, bricks, etc., and used them as starting materials for the synthesis of MoS_2. Most of the sulfided catalysts used in the petroleum industry are sulfurized from the oxide state at 400 °C. But the literature reports that at this temperature, the sulfidation is incomplete and the material obtained have a surface-covered structure and it may be easily oxidized to the parent material. Farag[31] and Okamato et al.[32] separately studied the sulfidation process at higher temperatures and confirmed that the sulfidation of molybdenum species were incomplete at 400 °C and it required a higher temperature. But high temperature sulfidation of the material increases the crystallinity as well as particle sizes of materials, which may reduce their catalytic and tribological performances. We prepared materials and sulfided at temperatures of 400 and 800 °C. Also, we synthesized MoS_2 using a hard templating method for comparison. The characteristics and tribological properties of the materials were studied and compared.

II. EXPERIMENTAL: MATERIALS AND METHODS

Ammonium heptamolybdate hexahydrate (99.98%) and acetyl acetonate (99%) were purchased from Merck India (Mumbai). Concentrated nitric acid (70%) and hydrofluoric acid (48%) were purchased from SD-Fine India (Bangalore). Deionized water used was obtained from Hi-Media laboratories. Commercial grade hydrogen and H_2S gas mixture were used for sulfidation. The precursors of MoS_2, micro- and nano-rods of molybdenum trioxide were synthesized by the hydrothermal route under autogenous pressure. Then the obtained materials were sulfided with a mixture of hydrogen sulfide and hydrogen gas. In a typical synthesis, 1 g ammonium heptamolybdate was dissolved in 50 mL deionized water and stirred for 30 min with 5 mL acetyl acetonate at 50 °C, then 50 mL concentrated HNO_3 was added drop wise. The mixture was kept stirring for 2 h at 50 °C, then transferred to a Teflon lined autoclave and kept for 48 h at 140 °C. The so-formed material was filtered and washed with distilled water till the pH was neutral and was dried overnight at 100 °C. Sulfidation of the material was carried out in a tubular reactor with 10% H_2S and 90% H_2 gas for 2 h at 400 °C (sample code: MNR) and 800 °C (sample code: MNNR). In the hard template method, mesoporous silica was used as the template and ammonium heptamolybdate was used as the molybdenum precursor. Wet impregnation method was used for the preparation of supported molybdenum trioxide and the sulfidation procedure was the same as above. The so-formed sulfided materials were treated with 1 molar HF for two hours, filtered, and dried at 100 °C to get silica-free MoS_2 (sample code: RM^2-3A).

The tribological properties of the materials were measured on a four-ball tribo-tester. The dry powder of synthesized MoS_2 and a lubricant grade commercial MoS_2 (3–5 μm particle size) were blended with commercial engine oil coded as CO-01. To attain a stable homogeneous dispersion during the blending process, 1% octadecylamine (ODA) was added into the blend. The presence of the surfactant prevents the nanoparticle to be agglomerated. The lubricant blends were prepared by addition of 0.5% by weight of synthesized MoS_2 and 1% by weight of ODA in CO-01. The characteristics of CO-01 are given in Table I. The tribological performance evaluation of the blends of lubricants was performed under the concentrated point-sliding contact on a four-ball tribo-tester. The ball test specimens with a hardness of 60 ± 2 HR and the

TABLE I. Physico-chemical properties of CO-01.

Lubricant	Flash Pt. °C, min.	Pour Pt. °C, min.	TAN, mg KOH/gm	Sulfated Ash, % by mass	Kin. viscosity at 40°C	Kin. viscosity at 100 °C	VI
CO–01	224	(−) 36	2.04	1.17	101.06	14.53	149

TAN-total acidity number; VI-viscosity index.

https://doi.org/10.1557/jmr.2013.178 Published online by Cambridge University Press

surface finish equivalent to N3 ~ N4 grade were fabricated from forged EN-31 steel. The tribological performance tests were conducted at a concentrated load of 392 N at 75 °C for 1 h duration. The rotational speed of the spindle was limited to 1200 rpm. The friction encountered in the contact during the entire duration of the test was recorded and the wear at the end of the test in the form of wear scar diameter was reported.

The physicochemical properties of the materials were characterized by x-ray diffraction (XRD), scanning electron microscopy (SEM), transmission electron microscopy (TEM), thermogravimetric analysis (TGA), and Fourier transform infra-red spectroscopy (FTIR). XRD patterns were obtained using Cu K_α radiation (40 kV and 40 mA, Bruker, Germany) with steps of 0.02° and a step time of 1 s. The SEM images were obtained on a field emission scanning electron microscope, FEI Quanta 200 F (10 or 30 kV). Materials were spread on a carbon tape prior to analysis. Energy-dispersive x-ray spectroscopy (EDX) was used for elemental analysis. The elemental mapping was conducted with the same spectrometer. The FTIR analysis was performed on Perkin Elmer 1760 X spectrometer (Singapore) with KBr pellets. TG analysis were conducted on a Perkin Elmer equipment under nitrogen with a ramping temperature of 10 °C/min. TEM analysis were conducted on a JEOL spectrometer at an acceleration voltage of 200 Kv. Prior to analysis, samples were dispersed in ethanol and sonicated for 5 min and dispersed on a copper grid.

III. RESULTS AND DISCUSSION

The crystallinity and phase structure of the synthesized materials were analyzed by XRD. Figure 1(a) shows the typical XRD patterns of the synthesized molybdenum trioxide nano-rods. The diffraction peaks in the image indicate that the so-formed material is highly crystalline with a clear orthorhombic phase (JCPDS 35-0609, $a = 0.3963$ nm, $b = 1.3856$ nm, $c = 0.3697$ nm, space group *Pbnm*), and the strong reflection peaks of $0k0$ ($k = 2, 4, 6$) confirmed that the material is in the preferred

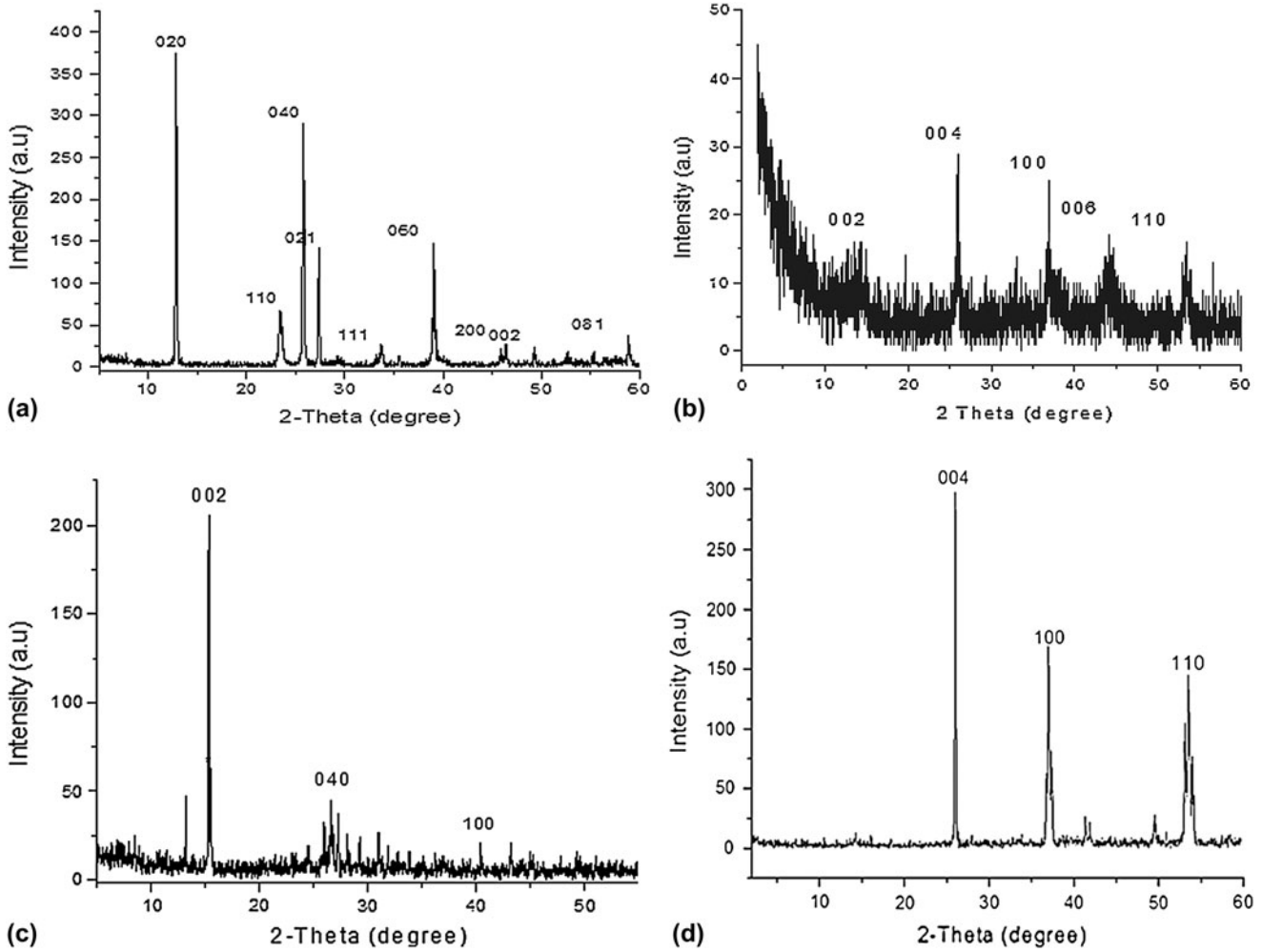


FIG. 1. XRD patterns of (a) MoO_3, (b) MoS_2, (c) MoS_2 (hard template) (d) sulfided at 800 °C.

https://doi.org/10.1557/jmr.2013.178 Published online by Cambridge University Press

crystallographic orientation.[33] The absence of any peaks corresponding to other phases shows that the synthesized material is a pure single phase. The diffraction pattern of MoS_2 is shown in Fig. 1(b). It shows that the crystallinity of the material decreased due to removal of the oxygen atoms from the lamellar MoO_3 structure. The wide diffraction peaks indicate that the material is nano-crystalline. Figure 1(c) shows a sharp diffraction pattern along 002 plane, indicating that the material synthesized with a hard template method is highly crystalline. The presence of weak peaks corresponding to MoO_3 indicates that some of the Mo–Oxygen bonds were stronger and remained, unlike in the case of the material synthesized by the hydrothermal method. Higher temperature sulfidation (800 °C) results in a completely sulfided crystalline phase [Fig. 1(d)], as also reported earlier,[24–29] but is more complicated and energy intensive for bulk practical application of such materials.

FTIR analysis of the MoO_3 and MoS_2 materials was carried out. Figure 2(a) shows the IR spectra of MoO_3. From the figure, it is clear that the material has various stretching and bending vibrations. A small peak at 3434 cm^{-1} might be due to OH groups of the absorbed water molecule, which is confirmed by the presence of bending mode of OH groups at 1631 cm^{-1}. The presence of terminal Mo=O bond is confirmed by a stretching vibration band at 995 cm^{-1}. The IR band at 877 cm^{-1} corresponds to the Mo–O–Mo bond stretching vibration in the material.[34] The stretching vibration of an oxygen atom linked to three molybdenum atoms was shown at 585 cm^{-1}. From Fig. 2(b), it is visualized that all the peaks corresponding to the oxygen linkages disappeared from the material after sulfidation. The bands at 964 and 722 cm^{-1} may correspond to the presence of Mo–S and Mo=S bonds.[35] From these results, it may be concluded that the final MoS_2 product obtained has no oxygen

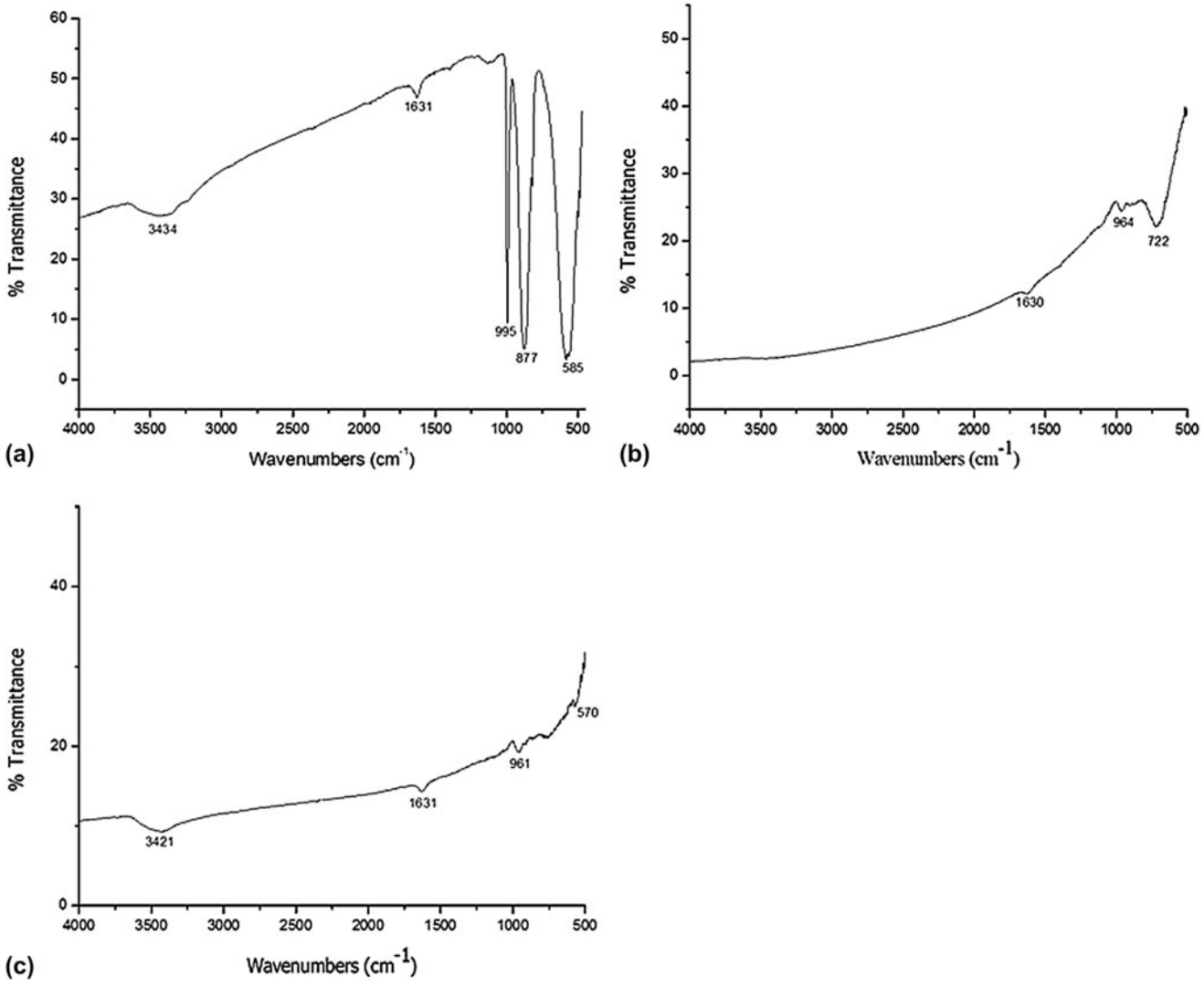


FIG. 2. FTIR patterns of (a) MoO_3, (b) MoS_2, and (c) MoS_2 (hard template).

https://doi.org/10.1557/jmr.2013.178 Published online by Cambridge University Press

atom i.e., all the oxygen atoms were replaced by sulfur atoms. Figure 2(c) represents the FTIR spectra of MoS_2 synthesized using a hard template. The absence of peaks corresponding to Si–O–Al and Si–O in the spectra reveals the complete removal of framework elements of the mesoporous silica (hard) template. The band at 961 cm^{-1} is related to Mo–S bonds.

Particle size distribution and morphology of the materials were studied using SEM. The SEM images of the synthesized materials are shown in Fig. 3. From these images, it can be observed that at different reaction conditions, the morphology of the materials was different. Reaction temperature and time of crystallization play a crucial role in controlling the crystallinity and particle agglomeration of the final product. Figure 3(a) shows that the molybdenum trioxide synthesis, at 70 °C with stirring for 2 h, produces hexagonal particles. With the same procedure but under autogeneous pressure for seven days and increasing the temperature from 70 to 80 °C, a material with a flower-like structure as shown in Fig. 3(b) was formed. Increasing the temperature to 120 °C and decreasing the crystallization time to 48 h resulted in the formation of rod-like structures [Fig. 3(c)] with slight agglomeration. When the temperature was further increased to 130 °C, the rod-like particles are less agglomerated [Fig. 3(d)]. Finally at 140 °C, perfect rods were obtained [Fig. 3(e)], confirming the effect of temperature on morphology. Figure 3(f) shows a clear, single-strand rod-like structures with length of several micrometers. At higher temperatures up to 240 °C, the so-formed materials do not have any notable difference compared with the material formed at 140 °C. The sulfided form of the nano-rods sustained their morphology after high temperature treatment with the corresponding gas mixture as shown in Fig. 3(g). Reconstruction of materials without changing

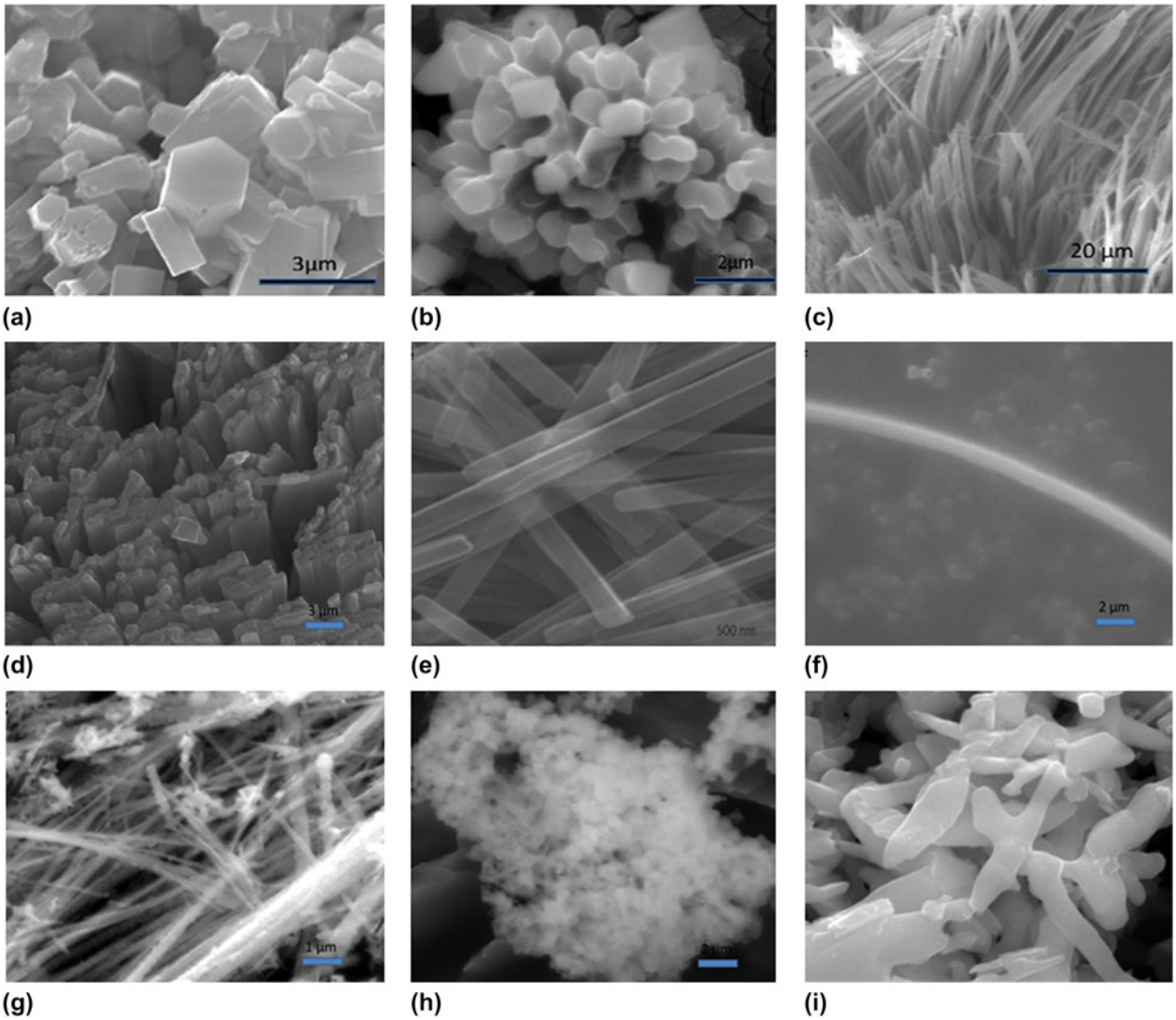


FIG. 3. SEM images of MoO_3 (a) 70 °C, (b) 80° C, 7 days, (c) 120° C, 48 h, (d) 130° C, 48 h, (e) 140 °C, (f) single strand MoO_3, (g) MoS_2, (h) MoS_2 (hard template), and (i) MoS_2 (sulfided at 800 °C).

https://doi.org/10.1557/jmr.2013.178 Published online by Cambridge University Press

the size and morphology is generally difficult in material synthesis. It is observed from Fig. 3(g) that the sulfidation process does not change the parent morphology of the material at 400 °C. It may be due to the interchange of sulfur with oxygen atoms without affecting the morphology and structure of the starting material. This results in the stacking of S–Mo–S layers in which, each molybdenum is bonded to four sulfur atoms that are arranged above the plane of the

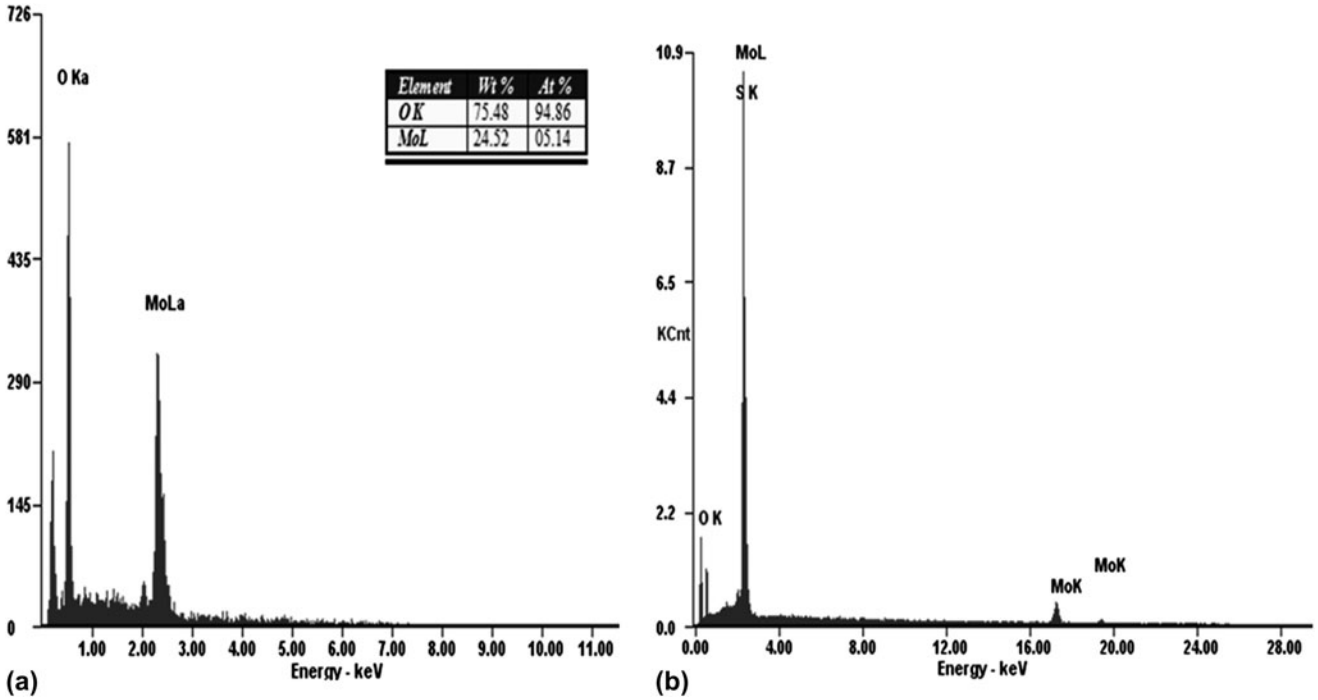


FIG. 4. EDS pattern of (a) MoO_3 and (b) MoS_2.

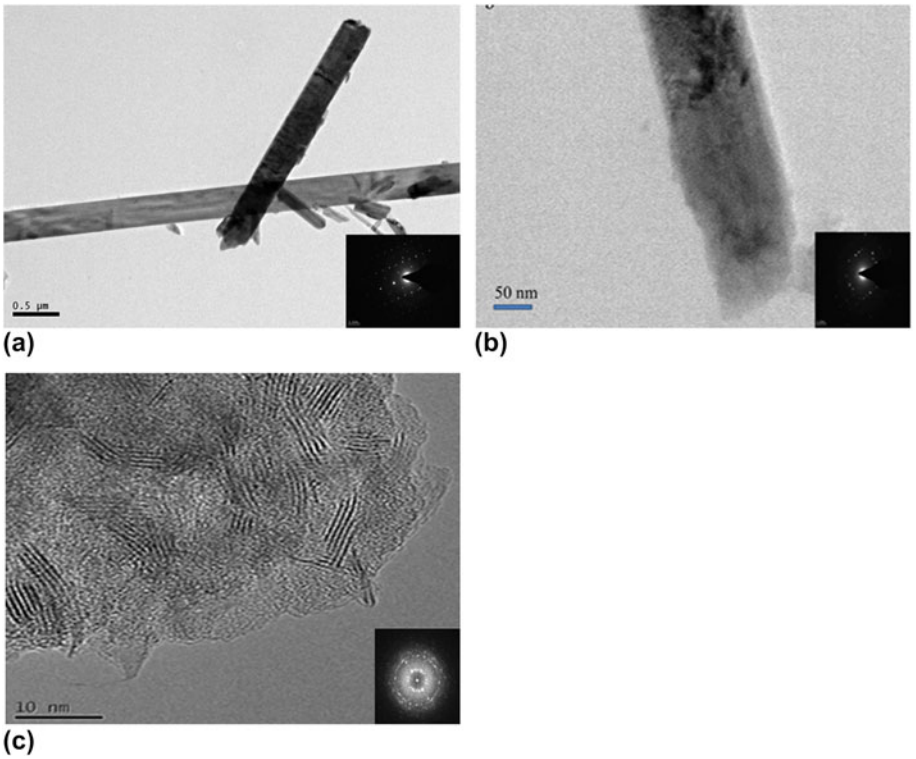


FIG. 5. TEM images of (a) MoO_3, (b) MoS_2, and (c) HRTEM of MoS_2 (hard template).

https://doi.org/10.1557/jmr.2013.178 Published online by Cambridge University Press

molybdenum layer[36] and thus, molybdenum can achieve full six-fold coordination by sulfur. But at higher sulfidation temperature [Fig. 3(i)], the stacking of the sulfur layer increased, and due to this, the material is agglomerated. Energy dispersive x-ray spectroscopy (EDS) patterns for MoS_2 (Fig. 4) show that oxide is almost completely converted to sulfide after sulfidation process. The elemental composition of the oxide material has a Mo:O ratio of 1:3. The electron diffraction of the K shell of molybdenum and the L shell of sulfur come under same energy region. Due to the overlapping of these energy levels, the percentage of sulfur was calculated by deleting the molybdenum energy level and it was 22%. The TEM and high resolution transmission electron microscope (HRTEM) images with selected area electron diffraction (SAED) patterns of the materials are shown in Figs. 5(a)–5(c). The rod-like molybdenum trioxide structure is clearly visualized in Fig. 5(a). Figure 5(b) is the TEM image of the corresponding molybdenum disulfide. The SAED pattern of the MoO_3 [Fig. 5(a), inset] shows the facets at an interval of less than 0.5 nm indicating that the arrangement of atoms in the material is well ordered and the material is well crystalline. But this arrangement is completely disordered after sulfidation. Figure 5(b) shows that the material is polycrystalline with crystal lattice planes of 100, 002, 110, etc. The HRTEM image of MoS_2 obtained by the hard templating route [Fig. 5(c)] shows multilayered nano-crystalline particles of sizes less than 10 nm. The corresponding SAED pattern of the material is shown in Fig. 5(c) (inset), which indicates that the material is also polycrystalline with clear 002 lattice plane.

Thermal stability of the material was studied by TG analysis in a nitrogen atmosphere. The results obtained are shown in supplementary information S1a–S1c. From these results, it is clear that the materials synthesized have high thermal stability. Figure S1(a) is the representative TG curve of pure MoO_3, and the sharp weight loss at 650 °C is due to the removal of oxygen from the frame work. There was no notable weight loss from MoS_2 nanorods [Fig. S1(b)]. MoS_2 synthesized using a hard template

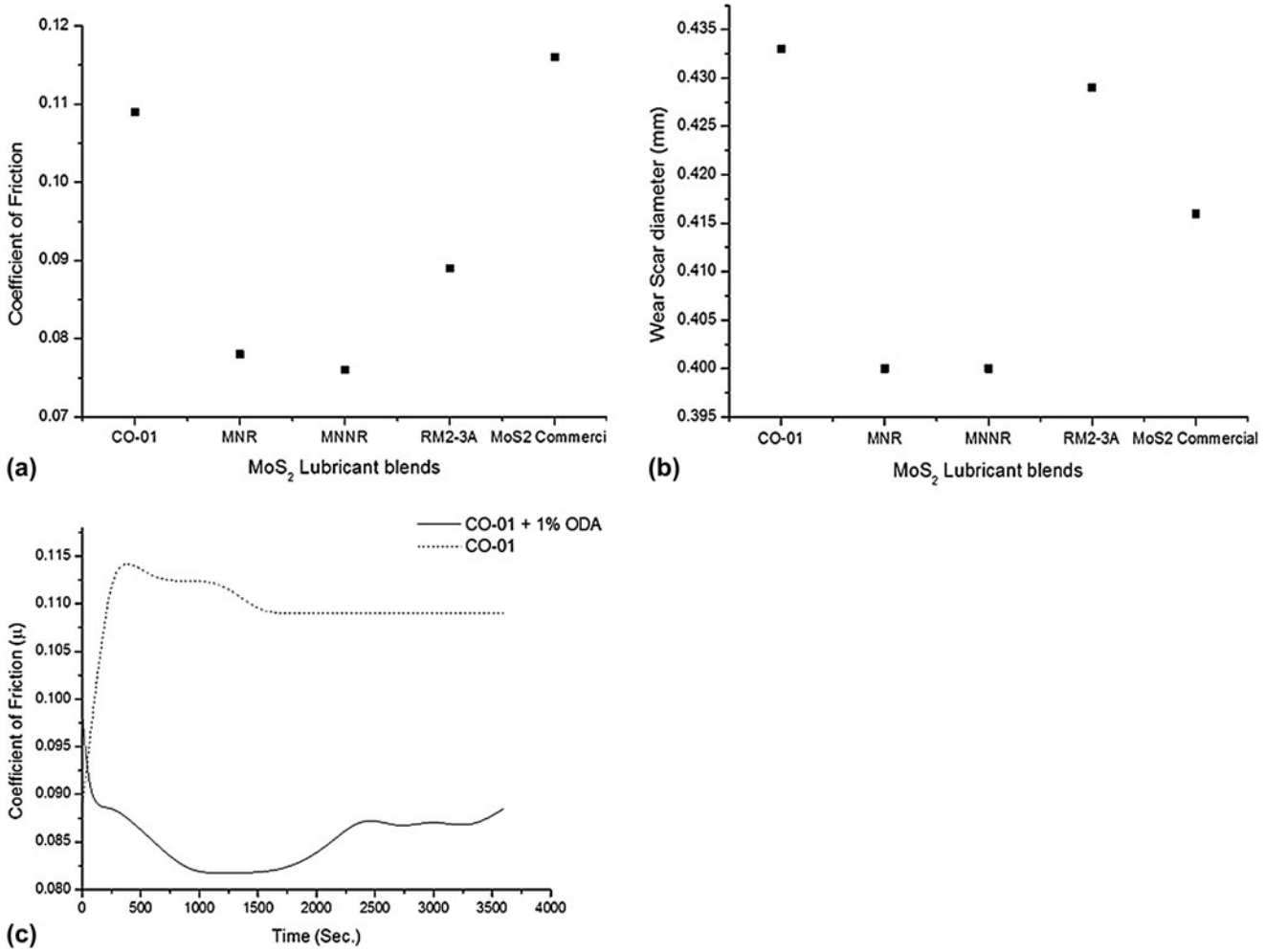


FIG. 6. Friction and antiwear behavior of lubricant blends.

https://doi.org/10.1557/jmr.2013.178 Published online by Cambridge University Press

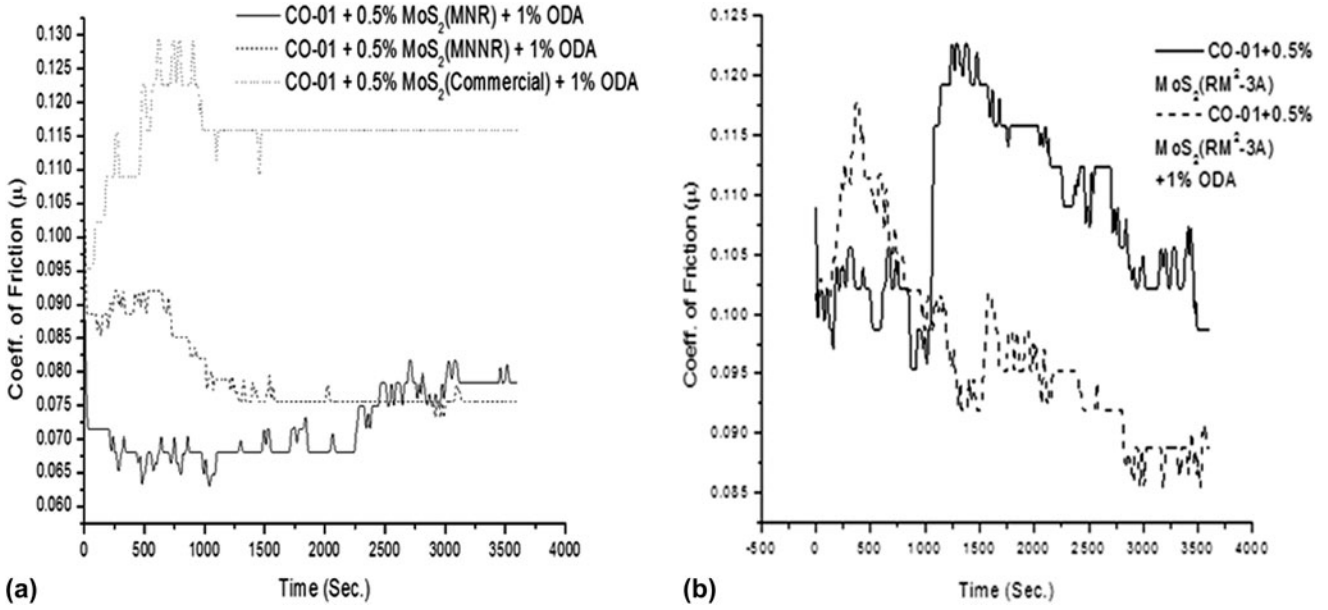


FIG. 7. Coefficient of friction characteristics against time of (a) MoS_2, sulfided at 400 °C (MNR) MoS_2, sulfided at 800 °C (MNNR) and commercial MoS_2 (b) MoS_2 (hard template).

also shows high thermal stability as shown in Fig. S1(c). A slight weight loss up to 400 °C may be due to the loss of moisture present in the sample.

Friction and antiwear behavior of the lubricant blends of the synthesized materials are shown in Fig. 6. The lubricant (CO-01) blended with synthesized MoS_2 and 1% octadecylamine surfactant (for dispersion) showed 20–30 times reduced friction and 2–8 times better antiwear behavior when compared with the performance of the unblended lubricant. From Fig. 7, it can be observed that samples MNNR and MNR (from hydrothermal route) show better friction reduction behavior and lower wear scar diameter than the crystalline sample, RM^2-3A (via hard templating route). It is also seen from Figs. 6 and 7 that the synthesized materials (MNNR and MNR) show better performance than commercial MoS_2 sample. The antiwear performance of the lubricant blends showed similar trends as that for friction, with MoS_2 sulfided at 400 (MNNR) and 800 °C (MNR), showing the least wear scar diameter of 0.04 mm. CO-01 + 1%ODA resulted in a wear scar diameter of 0.379 mm, which was 0.433 for only CO-01. The samples sulfurized at 400 °C (MNNR) showed slightly better overall performance than those sulfurized at 800 °C (MNR), which can be attributed to smaller less agglomerated MoS_2 particles at lower temperature. The experiments were conducted for 4000 s, and the result obtained is shown in Fig. 7. The higher frictional values at the beginning of the experiment were due to static friction that reduced in due course of time. The stabilized coefficient of friction i.e., the kinetic friction values for the blends were found to be lower for the MoS_2 rod-like material (MNR, MNNR) than for the MoS_2 nanoparticles obtained by the hard template route (RM^2-3A). This may be due to the structural differences of the two materials. The hard templated nanomaterial with <10-nm-size particles would show only interlayer sliding behavior, whereas the rod-like material synthesized by the hydrothermal method would give additional improvements, due to their structures. The hexagonal lamellar structure of MoS_2 results in the formation of thin boundary films on the surfaces under high loads thereby reducing the friction and the accompanied wear of the test specimens, on contact. Thus, the differences in the performances of the materials synthesized by the hydrothermal method [Fig. 7(a)] and hard template [Fig. 7(b)] were due to the differences in the crystallinity and morphology of the particles. The sulfidation temperature had little influence on the frictional behavior, but the blends with MoS_2 sulfided at 400 °C (MNR) stabilized much earlier as compared with other MoS_2 blends, and it may be due to the difference in morphology of the materials; the low temperature nano-rods [MNR, Fig. 3(g)] being better than high temperature agglomerates [MNNR, Fig. 3(i)].

IV. CONCLUSION

In summary, crystalline molybdenum trioxide rods, flowers, and bricks have been successfully synthesized by simple low temperature hydrothermal reactions. Compositional and morphological studies show that the parent material has an orthorhombic phase with linear Mo–O–Mo and Mo=O bonds. XRD and thermal studies confirmed that the material is crystalline and highly stable. The factors affecting the size and shape of the synthesized material were studied in detail. It can be concluded that during the hydrothermal synthesis, temperature and time are very important factors directing the size and morphology

https://doi.org/10.1557/jmr.2013.178 Published online by Cambridge University Press

of the material. Sulfidation of the as-synthesized material gives lamellar molybdenum disulfide nano-rods. Directly synthesized rod-like material gives better performance than the nanoparticles synthesized by the hard template method, in terms of friction coefficient and wear resistance properties. The synthesized molybdenum sulfide rods have high coefficient of friction reduction with excellent antiwear properties and so are promising as solid lubricants. The hard templated nanomaterial is also a promising one and it gives sliding friction reduction. The high stability of the material is an added advantage.

ACKNOWLEDGMENTS

Director, IIP is acknowledged for approving the work. MGS and BSR thank UGC and CSIR for research fellowship, respectively. The authors thank ASD of Indian Institute of Petroleum for analytical services.

REFERENCES

1. Z.X. Song, N. Minura, J.J. Bravo-Suaroz, T. Akita, S. Tsubota, and S.T. Oyama: Gas-phase epoxidation of propylene through radicals generated by silica-supported molybdenum oxide. *Appl. Catal., A* **316**, 142 (2007).
2. F. Wang and W. Ueda: Nanostructured molybdenum oxides and their catalytic performance in the alkylation of arenes. *Chem. Commun.* **0**, 3196 (2008).
3. L. Cheng, M.W. Shao, X.H. Wang, and H.B. Hu: Single-crystalline molybdenum trioxide nanoribbons: Photocatalytic, photoconductive, and electrochemical properties. *Chem. Eur. J.* **15**, 2310 (2009).
4. E. Comini, L. Yubao, Y. Brando, and G. Sberveglieri: Gas sensing properties of MoO_3 nanorods to CO and CH_3OH. *Chem. Phys. Lett.* **407**, 368 (2005).
5. X. Huang, Z. Zeng, and H. Zhang: Metal dichalcogenide nanosheets: Preparation, properties and applications. *Chem. Soc. Rev.* **42**, 1934 (2013).
6. N.J. Imonishi, K. Kanamura, and Z. Takehara: Synthesis of MoS_2 thin film by chemical vapor deposition method and discharge characteristics as a cathode of the lithium secondary battery. *J. Electrochem. Soc.* **139**, 2082 (1992).
7. D. Sun, W. Lu, D. Le, Q. Ma, M. Aminpour, M.A. Ortigoza, S. Bobek, J. Mann, J. Wyrick, T.S. Rahman, and L. Bartels: An MoSx structure with high affinity for adsorbate interaction. *Angew. Chem. Int. Ed.* **51**, 10284 (2012).
8. V.M. Mohan, H. Bin, and W. Chen: Enhancement of electrochemical properties of MoO_3 nanobelts electrode using PEG as surfactant for lithium battery. *J. Solid State Electrochem.* **14**, 1769 (2010).
9. S.M. Paek, J.H. Kang, H. Jung, S.J. Hwang, and J.H. Choy: Enhanced lithium storage capacity and cyclic performance of nanostructured TiO_2–MoO_3 hybrid electrode. *Chem. Commun.* **48**, 7536 (2009).
10. X. Zhang, B. Luster, A. Church, C. Muratore, A.A. Voevodin, P. Kohli, S. Aouadi, and S. Talapatra: Carbon nanotube-MoS_2 composites as solid lubricants. *Appl. Mater. Interface* **1**, 735 (2009).
11. R. Rosentsveig, A. Margolin, A. Gorodnev, R. Popovitz-Biro, Y. Feldman, L. Rapoport, Y. Novema, G. Naveh, and R. Tenne: Synthesis of fullerene-like MoS_2 nanoparticles and their tribological behavior. *J. Mater. Chem.* **19**, 4368 (2009).
12. V.G. Pol, S.V. Pol, and A. Gedanken: Micro to nano conversion: A one-step, environmentally friendly, solid state, bulk fabrication of WS_2 and MoS_2 nanoplates. *Cryst. Growth Des.* **8**, 1126 (2008).
13. A. Zak, Y. Feldman, V. Lyakhovitskaya, G. Leitus, R. Popovitz-Biro, E. Wachtel, H. Cohen, S. Reich, and R. Tenne: Alkali metal intercalated fullerene-like MS_2 (M = W, Mo) nanoparticles and their properties. *J. Am. Chem. Soc.* **124**, 4747 (2002).
14. M. Remskar, Z. Skraba, P. Stadelmann, and F. Levy: Structural stabilization of new compounds: MoS_2 and WS_2 micro- and nanotubes alloyed with gold and silver. *Adv. Mater.* **12**, 814 (2000).
15. M. Chhowalla, A. Gehan, and J. Amaratunga: Thin films of fullerene-like MoS_2 nanoparticles with ultra-low friction and wear. *Nature* **407**, 164 (2000).
16. B. Hu, L. Mai, W. Chen, and F. Yang: From MoO_3 nanobelts to MoO_2 nanorods: Structure transformation and electrical transport. *ACS Nano* **3**, 478 (2009).
17. Z. Wang, H. Wang, C. Yang, and J. Wu: Synthesis of molybdenum oxide hollow microspheres by ethanol and PEG assisting hydrothermal process. *Mater. Lett.* **64**, 2170 (2010).
18. T. Xia, Q. Li, X. Liu, J. Meng, and X. Cao: Morphology-controllable synthesis and characterization of single-crystal molybdenum trioxide. *J. Phys. Chem. B* **110**, 2006 (2006).
19. Y. Tian, X. Zhao, L. Shen, F. Meng, L. Tang, Y. Deng, and Z. Wang: Synthesis of amorphous MoS_2 nanospheres by hydrothermal reaction. *Mater. Lett.* **60**, 527 (2006).
20. M. Bar-Sadan, A.N. Enyashin, S. Gemming, R. Popovitz-Biro, S.Y. Hong, P. Yehiam, R. Tenne, and G. Seifert: Structure and stability of molybdenum sulfide fullerenes. *J. Phys. Chem. B* **110**, 25399 (2006).
21. Z.H. Wen, Q. Wang, and J.H. Li: Electrochemical behavior of -MoO_3 nanorods as cathode materials for rechargeable lithium batteries. *Nanosci. Nanotechnol.* **6**, 2117 (2006).
22. F. Dury, V. Misplon, and E.M. Gaigneaux: Probing the reduction state of Mo oxide catalysts by the deoxygenation of carboxylic acid. *Catal. Today* **91**, 111 (2004).
23. D. Chen, M. Liu, L. Yin, T. Li, Z. Yang, X. Li, B. Fan, H. Wang, R. Zhang, Z. Li, H. Xu, H. Lu, D. Yang, J. Sun, and L. Gao: Single-crystalline MoO_3 nanoplates: Topochemical synthesis and enhanced ethanol-sensing performance. *J. Mater. Chem.* **21**, 9332 (2011).
24. L.Q. Mai, B. Hu, W. Chen, Y.Y. Qi, C.S. Lao, R.S. Yang, Y. Dai, and Z.L. Wang: Lithiated MoO_3 nanobelts with greatly improved performance for lithium batteries. *Adv. Mater.* **19**, 3712 (2007).
25. J. Zhou, N.S. Xu, S.Z. Deng, J. Chen, J. C. She, and Z. Wang: Large-area nanowire arrays of molybdenum and molybdenum oxides: Synthesis and field emission properties. *Adv. Mater.* **15**, 1835 (2003).
26. T. Siciliano, A. Tepore, E. Filippo, G. Micocci, and M. Tepore: Characteristics of molybdenum trioxide nanobelts prepared by thermal evaporation technique. *Mater. Chem. Phys.* **114**, 687 (2009).
27. K. Kalantar-zadeh, J. Tang, M. Wang, K.L. Wang, A. Shailos, K. Galatsis, R. Kojima, V. Strong, A. Lech, W. Wlodarski, and R.B. Kaner: Synthesis of nanometre-thick MoO_3 sheets. *Nanoscale* **2**, 429 (2010).
28. C.V. Krishnan, J. Chen, C. Burger, and B. Chu: Polymer-assisted growth of molybdenum oxide whiskers via a sonochemical process. *J. Phys. Chem. B* **110**, 20182 (2006).
29. G. Pan, Q. Guo, Z. Zhao, S. Zhouwang, Y. Qin, and L. Wang: Tribological properties of solid multilayer composite coatings in dry rolling contact. *Tribol. Int.* **44**, 789 (2011).
30. X. Zhou, D. Wu, H. Shi, X. Fu, Z. Hu, X. Wang, and F. Yan: Study on the tribological properties of surfactant-modified MoS_2 micrometer spheres as an additive in liquid paraffin. *Tribol. Int.* **40**, 863 (2007).

https://doi.org/10.1557/jmr.2013.178 Published online by Cambridge University Press

31. H. Farag: Effect of sulfidation temperatures on the bulk structures of various molybdenum precursors. *Energy Fuels* **16**, 944 (2002).
32. Y. Okamoto, A. Kato, Usman, N. Rinaldi, T. Fujikawa, H. Koshika, I. Hiromitsu, and T. Kubota: Effect of sulfidation temperature on the intrinsic activity of Co–MoS_2 and Co–WS_2 hydrodesulfurization catalysts. *J. Catal.* **265**, 216 (2009).
33. F. Fang, Y. Shu, A. Wang, and T. Zhang: Green synthesis and characterization of anisotropic uniform single-crystal α-MoO_3 nanostructures. *J. Phys. Chem. C* **111**, 2401 (2007).
34. G.S. Zakharova, C. Taeschner, V.L. Volkov, I. Hellman, R. Klingeler, A. Leonhardt, and B. Buechner: $MoO_{3-\delta}$ nanorods: Synthesis, characterization and magnetic properties. *Solid State Sci.* **9**, 1028 (2007).
35. F.L. Pua, C.H. China, S. Zakaria, T. Liew, M.A. Yarmo, and N.M. Huang: Simple hydrothermal route for synthesizing transition metal sulfide nanoparticle. *Sains Malaysiana* **39**, 243 (2010).
36. L.P. Hansen, Q.M. Ramasse, C. Kisielowski, M. Brorson, E. Johnson, H. Topsøe, and S. Helveg: Atomic-scale edge structures on industrial-style MoS_2 nanocatalysts. *Angew. Chem. Int. Ed.* **50**, 10153 (2011).

Supplementary Material

Supplementary materials can be viewed in this issue of the *Journal of Materials Research* by visiting http://journals.cambridge.org/jmr.

https://doi.org/10.1557/jmr.2013.178 Published online by Cambridge University Press